Slope water intrusions onto Georges Bank

James H. Churchill
Department of Physical Oceanography, Woods Hole Oceanographic Institution, Woods Hole, Massachusetts, USA

James P. Manning
National Marine Fisheries Service, National Oceanic and Atmospheric Administration, Woods Hole, Massachusetts, USA

Robert C. Beardsley
Department of Physical Oceanography, Woods Hole Oceanographic Institution, Woods Hole, Massachusetts, USA

Received 25 March 2002; revised 6 August 2003; accepted 24 September 2003; published 18 November 2003.

[1] Data from moored instruments and hydrographic cruises of the U.S. GLOBEC NW Atlantic/Georges Bank program reveal a series of intrusions of high-salinity water extending onto the southern flank of Georges Bank during the spring and summer of 1995. On the basis of the layer of maximum salinity, these intrusions may be divided into three different types: near surface, near bottom, and pycnocline. The water mass and flow structure of all intrusions are highly variable, owing partly to wind-driven motions and partly to meanders and eddies formed along the front of the intruding water. The mooring data of May clearly show the passage of two cyclonic features, each with a core of intruding water. While the intrusions are shown to dominate the flux of high-salinity water onto the southern flank, the data examined offer no evidence that intrusions enhance nutrient concentrations over the southern flank. *INDEX TERMS:* 4223 Oceanography: General: Descriptive and regional oceanography; 4528 Oceanography: Physical: Fronts and jets; 4219 Oceanography: General: Continental shelf processes; *KEYWORDS:* shelf-edge exchange, slope water intrusions, intrusions onto Georges Bank

Citation: Churchill, J. H., J. P. Manning, and R. C Beardsley, Slope water intrusions onto Georges Bank, *J. Geophys. Res.*, *108*(C11), 8012, doi:10.1029/2002JC001400, 2003.

1. Introduction

[2] The waters over the Middle Atlantic Bight (MAB) shelf and the southern flank of Georges Bank are separated from the warmer and more saline waters offshore by a well-defined surface-to-bottom front. Although this front is a persistent feature at the shelf edge and upper slope, it is not impenetrable. There are numerous observations of shelf water transport seaward of the front and of intrusions of slope water onshore of the front. Both types of intrusions can have significant ecological consequences. Slope water intrusions, for example, may carry expatriate species of zooplankton and larval fish onto the MAB shelf and Georges Bank [*Hare and Cowen*, 1991, 1996].

[3] Hydrographic data have revealed at least two distinct types of slope water intrusions. Data acquired during the time of year when shelf water is vertically stratified (typically May–November) often show slope water extending shoreward onto the shelf within the seasonal pycnocline. Evidenced by a vertical salinity maximum, this sort of intrusion is usually seen between depths of 10 and 40 m [*Boicourt and Hacker*, 1976; *Gordon and Aikman*, 1981; *Houghton and Marra*, 1983; *Churchill et al.*, 1986]. Hydrographic and moored instrument data have also revealed intrusions of slope water within near-bottom layers over the MAB shelf. The limited observations of these features suggest that their appearance may be largely confined to the period when shelf waters are vertically well mixed [*Houghton et al.*, 1994; *Churchill and Aikman*, 1996].

[4] Using hydrographic measurements and data from moored acoustic Doppler current profilers (ADCPs), *Flagg et al.* [1994] carried out an in-depth study of pycnocline intrusions seen east of Virginia in the summer of 1988. They found that these intrusions can be generated very rapidly, over periods of a few days, by local cross-shelf currents. Employing the same data, *Houghton et al.* [1994] examined near-bottom frontal motions and identified lengthy near-bottom excursions of slope water onto the shelf. These also appeared on short timescales (order days) and were confined to the period when shelf waters were vertically unstratified.

[5] The principal driving mechanisms of slope water intrusions have yet to be fully identified. *Flagg et al.* [1994] and *Houghton et al.* [1994] found that upwelling-favorable winds tended to coincide with pycnocline and near-bottom intrusions. However, *Flagg et al.* [1994] determined that wind forcing alone could not account for the transport responsible for the pycnocline intrusions they observed.

[6] In this paper, we examine a series of slope water intrusions that appeared over the southern flank of Georges Bank during the spring and summer of 1995. During this

0148-0227/03/2002JC001400$09.00

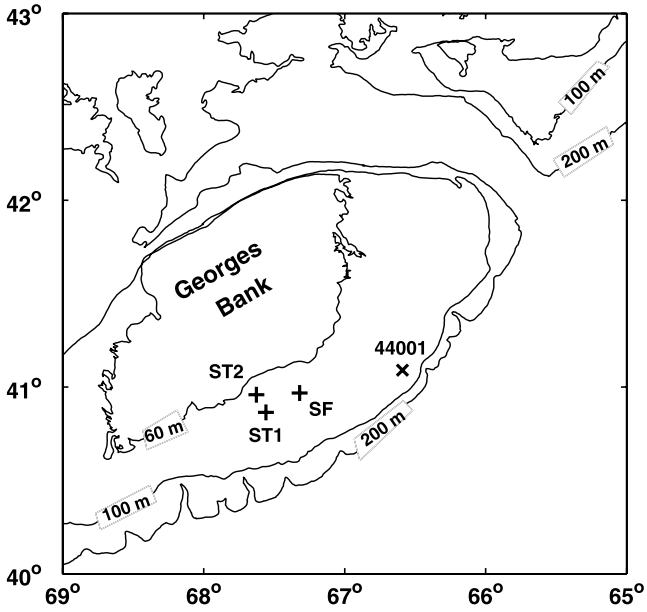

Figure 1. Georges Bank with the locations of the study's mooring sites (pluses) and NOAA environmental buoy 44001 (cross).

period, water over the Bank was intensively sampled as part of the Stratification Study of the U.S. Global Ocean Ecosystems Dynamics (GLOBEC) Northwest Atlantic/ Georges Bank program. Using the measurements acquired (section 2), we examine the hydrographic and flow structure of the intrusions (sections 3.1, 3.3, and 4.2), discuss their appearance in the sea surface temperature field (section 3.2), estimate their potential nutrient load (section 4.1), assess their influence on cross-margin salt transport (section 4.3), and examine their relation to wind-forced motions (section 4.4). We also consider our findings in light of results from recent modeling and biological studies (section 5).

2. Measurements

[7] The time series data used in this study came from moored instruments set out at three sites over Georges Bank's southern flank, roughly defined as the region of southern Georges Bank between the 60- and 100-m isobaths (Figure 1). Designated as ST1, ST2, and SF, these mooring sites were situated so that the data acquired could resolve both along-bank and across-bank gradients. One mooring site pair (ST1 and ST2) was oriented along a line perpendicular to the local isobaths, while a second pair (ST1 and SF) was situated on the 76-m isobath (see Table 1 for details of the records obtained at each mooring site).

[8] Owing to a number of factors, the period over which data were recorded varied from site to site (Table 1). Instruments were deployed at ST1 and ST2 in early February 1995. At ST1, all instruments remained intact throughout the deployment period and were recovered in late August 1995. However, data acquisition at ST2 was cut short on July 27 when the upper portion of the mooring was evidently severed by a passing trawler. Two months later, this portion of the mooring was recovered, with most instruments intact, by a fisherman near Hudson Canyon. Recovery of the mooring's lower portion occurred on schedule in late August. Instruments at SF were also cut free by fishing activity, causing a nearly 2-month hiatus in data acquisition at the site. The records from SF used in our study were from the deployment following this hiatus. Unfortunately, these did not include velocity records. An acoustic Doppler current profiler (ADCP) was deployed at the site, but produced only a few days of data due to hardware and software problems.

[9] Unless otherwise noted, all time series shown here have been low-pass-filtered with a 50-hour half-power period filter to eliminate most of the vigorous tidal signal characteristic of records from Georges Bank. Velocities have been rotated into a local coordinate system with the along-bank axis directed toward 51°T. This orientation, roughly aligned with the local isobaths, was chosen such that the depth-averaged mean cross-bank flow determined from the ST1 data was close to zero.

[10] Most of the wind velocity data used in our study came from a vector-averaging wind recorder (VAWR) [*Dean and Beardsley*, 1988] placed on a surface buoy at ST1. Owing to instrument failure, the wind record from this sensor had a 40-day gap (June 1 to July 10). This was filled using the wind data from NOAA buoy 44011, which was 87 km east of ST1 (Figure 1). The first step of the filling procedure was to use the 122 days of overlapping 44001 and ST1 wind data to derive a vector regression function, with an optimal time shift, relating the two wind velocity series. This function was then applied to the 44011 velocity series to fill the ST1 velocity record gap. Further details of

Table 1. Periods and Locations of Moored Temperature, Salinity, and Velocity Measurements Used in This Study[a]

Site	Location	Water Depth, m	Period 1995	Depths, m		
				Temperature	Salinity	Velocity
ST1	40.86°N 67.56°W	76	Jan. 23 to Aug. 23	1.0, 1.5, 2.0, 3.5, 5.6, 6.3, 8.0, 10.5, 11.1, 12.8, 14.5, 19.5, 22.5, 26.1, 28.8, 31.5, 37.5, 40.8, 46.0, 46.6, 61.5, 64.5, 65.1, 67.5	1.5, 6.3, 11.1, 26.1, 46.6, 65.1	5.2, 7.5, 10.0, 14.0, 19.0, 25.0, 25.0, 31.0, 37.0, 45.5, 64.0, 70.0
ST2	40.96°N 67.63°W	68	Feb. 3 to Aug. 5	1.0, 5.4, 11.0, 17.0, 26.1, 32.0, 37.7, 42.8, 61.5	1.0, 11.0, 32.0, 61.5	15.0, 35.0, 62.0
SF	40.97°N 67.32°W	75	Feb. 3 to March 4 and April 26 to Aug. 23	1.0, 5.0, 10.0, 15.0, 20.0, 25.0, 30.0, 35.0, 40.0, 45.0, 50.0	5.0, 10.0, 15.0, 20.0, 25.0, 30.0, 35.0, 40.0, 45.0, 50.0	no data

[a]Further details of the measurements at these sites, including additional properties measured, are given by *Alessi et al.* [2001].

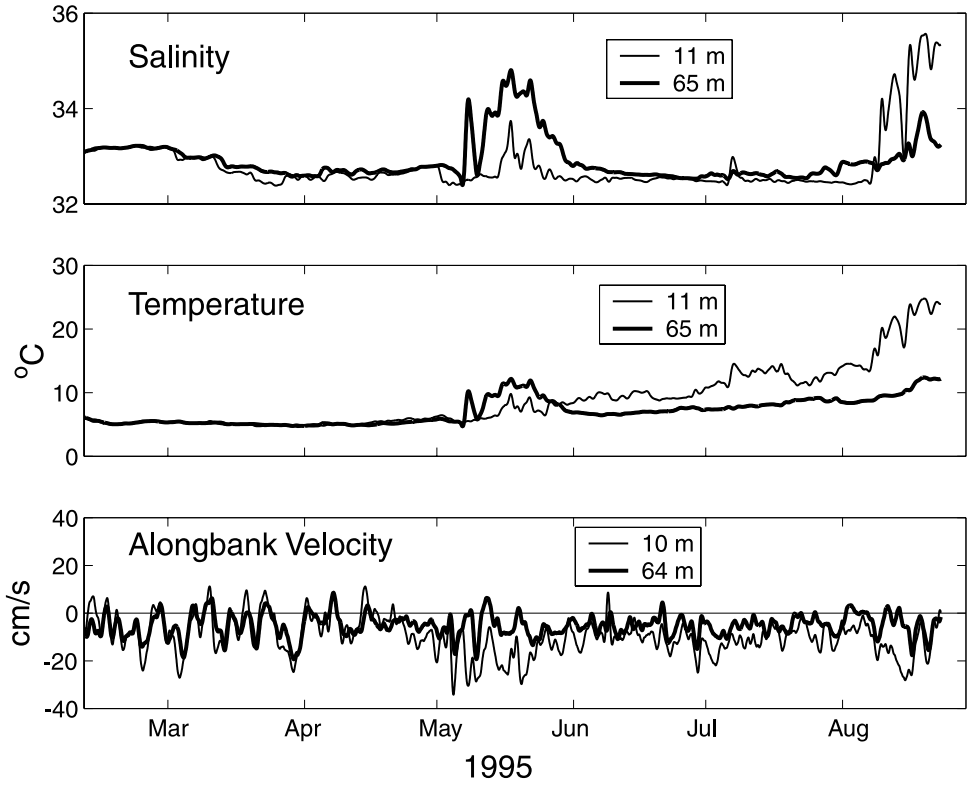

Figure 2. Low-pass filtered time series of salinity, temperature, and along-bank velocity measured at the indicated depths at ST1.

this procedure are given by *Alessi et al.* [2001]. Wind velocity was converted to surface wind stress using the TOGA/COARE (version 2.5) formulation (see *Beardsley et al.* [2003] for details).

[11] Our study also employed shipboard CTD and ADCP data. The tidal signal was removed from the ADCP velocities using the algorithm of M. Dunn (personal communication, 2000). This model determined the tidal velocity at any location and time on Georges Bank using Gaussian basis functions [*Flagg and Dunn*, 2003]. The coefficients of these functions were determined at nodal points by least squares fitting of velocity data.

3. Observations

3.1. Time Series

[12] Selected low-pass-filtered time series of temperature and salinity from ST1 clearly show the presence of anomalously warm and saline water intruding onto the southern flank (Figure 2). Before discussing these intrusions, it is useful to set forth some water mass definitions. One is ''resident'' southern flank water, defined here as water residing over the southern flank, onbank of the bank-edge front, during the time of our study. On the basis of the ST1 salinity records, this water is deemed to have salinities of 32.5 and less. Other water masses to consider are waters within the bank-edge front and slope water. The CTD data acquired over April–August 1995 (some of which are presented in section 3.3), indicate that the bank-edge front spans salinities of 33–35, and slope water occurs at salinity greater than 35. These definitions, specific to our study period, are not significantly different from those derived from historical data by *Lentz et al.* [2003]. In their classification scheme, bank-edge frontal water extends over a 33.6–35 salinity range and slope water has salinities greater than 35.

[13] In the ST1 salinity records, significant intrusions of offbank water, identified by salinities in excess of 33, appear during May and August. As deduced from the temperature and salinity records, the character of May and August intrusions differs significantly. In May, the temperature and salinity of the intruding water steadily increase going toward the bottom. By contrast, the August intrusion appears to be principally a near-surface feature, with temperature and salinity tending to decrease with depth. A third intrusion of relatively saline water appears in early July. In the low-pass filtered salinity series from ST1, this is evidenced by a 0.6 increase in salinity (Figure 2). The actual salinity increase due to the intrusion, seen in the unfiltered salinity records (not shown), is near 1.0. All intrusions occur at a time when the along-bank flow over the southern flank is predominantly to the southwest (Figure 2) and of order 10 cm s^{-1} in magnitude. Rapid along-shelf advection of the intruding water, of order 10 km d^{-1}, would thus be expected.

[14] This advection, combined with the small along-bank scale of the intrusions, may be in part responsible for the large temporal variations in salinity seen in the ST1 and SF records during May and August, evidenced here by contours of the ST1 and SF salinities on a time-depth surface (Figures 3 and 4). Significant differences in the ST1 versus SF salinities during May and August offer

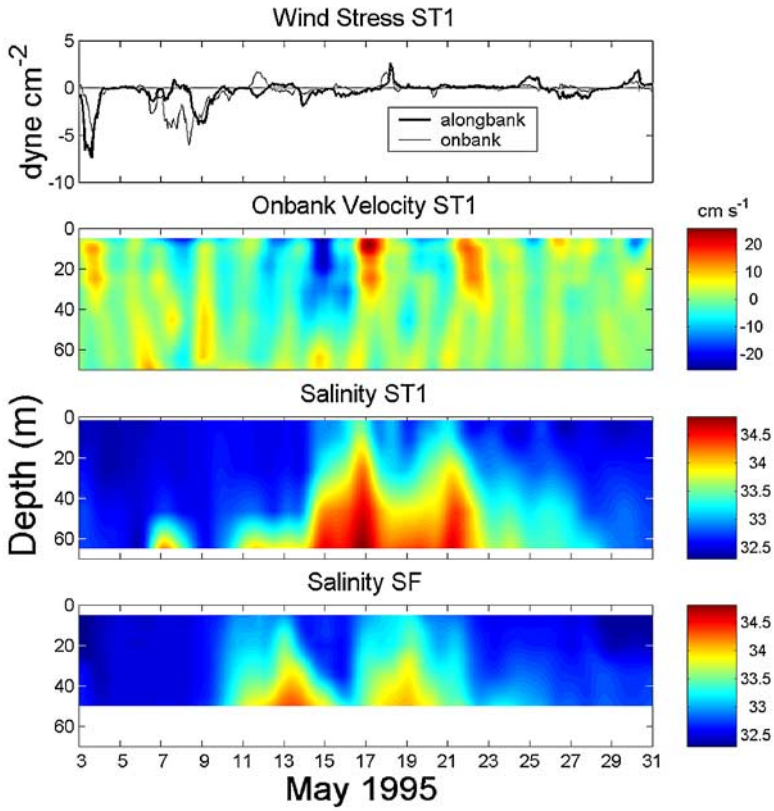

Figure 3. Wind stress and water properties at ST1 and SF during May 1995. In the top panel, alongbank wind stress is positive to the east-northeast (at 51°T) and onbank wind stress is positive to the north-northwest. Onbank velocity (second panel) follows the same convention. Time is in GMT.

further evidence that the intruding water seen during these months consisted of features with relatively small along-bank scales (of order, or less than, the site separation of 23 km).

[15] The first indication of intruding water in the May ST1 salinity record takes the form of a brief near-bottom intrusion of high-salinity water, extending no higher than 50 m depth and appearing over May 7–9 (Figure 3). This is followed by a second near-bottom saline intrusion, of similar vertical extent, appearing first on May 11. However, the dominant features of the May salinity records from ST1 and SF appear to be caused by two separate intrusions, extending over most of the water column and with a steady salinity increase toward the bottom. These intrusions produce temporal maxima in the ST1 salinities on May 16 and May 21. The salinity records at SF reveal intrusions with similar characteristics, but with maximum salinities occurring at earlier times: on May 13 and May 19. The successive appearance of each salinity maximum, first at SF and then at ST1, indicates a southwestward translation of intrusions. For each intrusion, the rate of translation may be roughly determined as the ratio of the distance separating SF and ST1 to the time difference between the appearance of the salinity maximum at the two sites. Following this approach, southwestward translation rates of 7.8 and 12.5 cm s^{-1} are determined for the first and second intrusion, respectively. The latter translation rate is close to the vertically and temporally averaged along-bank velocity measured at ST1 during mid-May (roughly 12 cm s^{-1}).

[16] The ST1 and SF salinity records of August reveal a series of near-surface intrusions with complicated spatial and temporal variations (Figure 4). At both sites, intruding water first appears early on August 9. Afterward, however, the salinities seen at the two sites show little similarity. Most notable are several periods when intruding water, evidenced by salinity >34, appears at one mooring, while resident southern flank water, with salinity <32.5, is seen at the other. The vertical salinity structure of the intruding water also shows significant temporal variation. At times, the intruding water is nearly homogeneous over its full vertical extent (surface 20–30 m), whereas at other times, it contains a well-defined vertical salinity maximum, usually at ~15 m.

3.2. Evidence From Sea Surface Temperature Imagery

[17] In agreement with the above time series observations, images of sea surface temperature (SST), derived from satellite radiometer measurements, reveal a series of small-scale intrusions of warm offbank water extending onto the southern flank during May and August 1995 (Figure 5). Many of these features have a form suggestive of a frontal instability or frontal eddy. In addition, some images from May and August show what appear to be detached, or nearly detached, parcels of warm water extending well onto the southern flank. Three examples are shown here. The first is a nearly circular patch of warm water that appears in the images of May 6–7. In these images, the patch appears to be moving toward the west, with its center

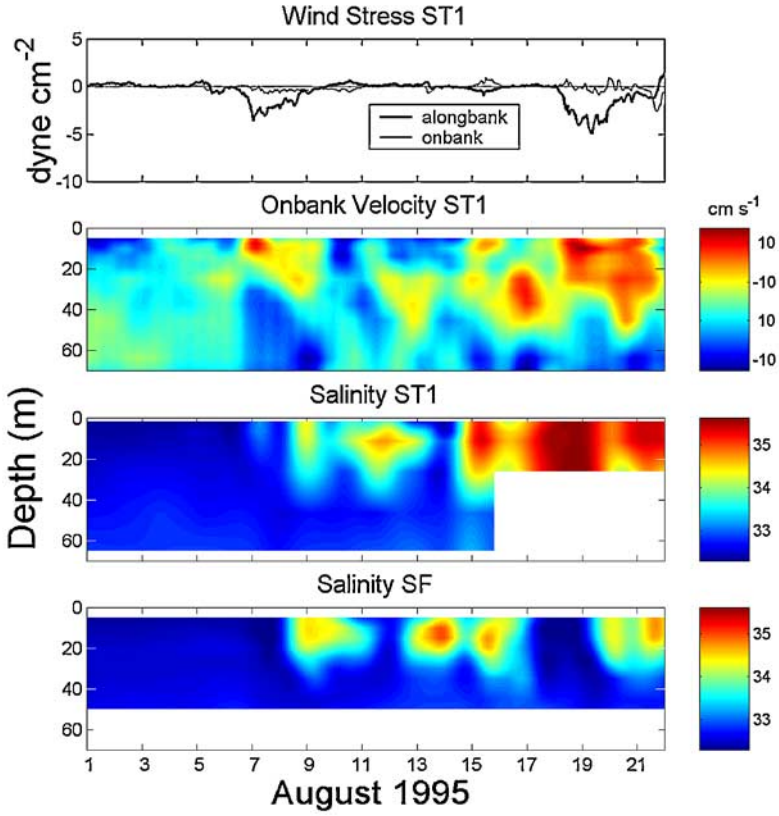

Figure 4. Same as Figure 3 except showing wind stress and water properties at ST1 and SF during August 1995.

roughly following the 85-m isobath. On May 6 (Figure 6a), it is centered at roughly 40°51′N, 67°25′W. The second example is what appears to be a series of eddies generated by frontal instabilities. These are evident in the images of May 14–15 (Figure 6b). The third example is a pair of eddies extending to the 60-m isobath. In an image from May 20 (Figure 6c), these are silhouetted by warm water bands apparently drawn onbank from an intrusion of warm surface water that extends to the 80-m isobath. The temperature contrast of these bands relative to the surrounding water is small (~1°C). These bands are no longer distinguishable in images after 1200 UTC May 21.

[18] The SST images also show the presence of a Gulf Stream warm-core ring impinging on the eastern portion of the southern flank during the time periods of all the intrusions considered here. The ring appearing during the time of the May intrusions (Figure 5a) first appears off the southern flank in mid-April. In the SST images, it appears to move steadily to the WSW, reaching the offing of the Great South Channel by mid-June. The ring appearing during the times of the July and August intrusions (Figure 5b) makes a much slower transit of the Bank region. It appears off the Northeast Channel in early July and is only about 400 km to the WSW by early November. The SST imagery also shows both rings vigorously interacting with the Gulf Stream while transiting the southern flank.

3.3. Temperature-Salinity Properties

[19] The temperature-salinity (T-S) properties of the intruding waters offer evidence of their origins. As revealed by data from the moored sensors, the intrusions of May, July, and August each have distinct T-S properties (Figure 7). The May intrusions are formed by relatively cold and saline water. The T-S properties of this water are tightly scattered along a nearly straight line (Figure 7, top). The high-salinity portion of this line falls within the range of T-S characteristics typically found in subsurface slope water residing off the southern flank during spring as defined by the analysis of historical data by *Flagg* [1987].

[20] Most of the intruding water seen in August is of relatively high temperature. The T-S properties of this water are broadly scattered about line with endpoints at roughly 15°C, 33 and 25°C, 35.6. At salinities greater than 35, they fall within the range of T-S properties typical of surface (0–50 m) slope water found off the southern flank [*Flagg*, 1987]. Measurements from 65 m depth at ST1 reveal what appears to be a second type of high-salinity water intruding onto the southern flank during late August (Figure 2). Its T-S characteristics are scattered about a line roughly centered at 11.5°C and extending to a salinity of 34.1 (Figure 7, bottom left).

[21] The maximum salinity measured within the July intrusion is 33.6 and occurs at 16°C. On the basis of hydrographic data acquired in the late spring and summer of 1995, this is characteristic of water found within the onbank portion of the bank-edge front. Conforming with the characteristics of the pycnocline intrusions discussed in section 1, this intrusion appears over the full range of the pycnocline, spanning depths of 10–30 m, and is bracketed above and below by less saline water. Although this feature

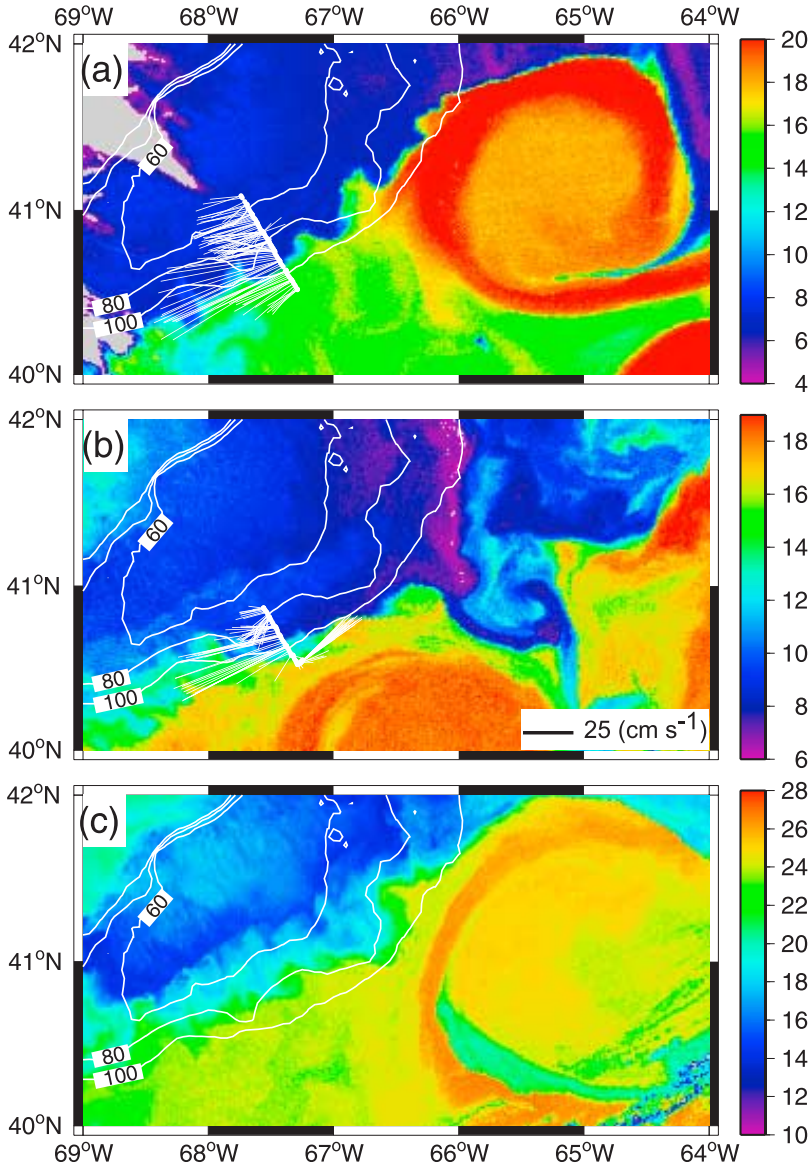

Figure 5. Sea surface temperature images of the Georges Bank region on (a) May 5, (b) May 28, and (c) August 13, 1995. The velocity vectors are "detided" ADCP velocities at 20 m derived from shipboard measurements acquired on May 4 (Figure 5a) and May 29 (Figure 5b).

is interesting as an example of a pycnocline intrusion, the focus of the analysis to follow will be on the May and August intrusions as these contained fluid clearly identified as slope water.

4. Analysis

4.1. Nutrient Concentrations Within Intrusions

[22] When considering the possible effects of intrusions on productivity over the bank, a critical issue is the extent to which the intrusions supply new nutrients to the bank. Unfortunately, there are no nutrient measurements within the intrusions of 1995. However, a sense of the nutrient concentrations within these intrusions may be gained by comparing their T-S properties with the T-S-nutrient relationships obtained using data from other periods. We have derived T-S-nutrient relationships using the nutrient and CTD data acquired over the southern flank and adjacent slope during 15 GLOBEC cruises conducted over 1997–1999. All cruises were carried out during the months of January through June. The T-S-nutrient relationships derived from these data are exemplified here by a contour plot of nitrate plus nitrite concentration on a T-S surface (Figure 8). Revealed by this plot is a tendency for nitrate plus nitrite concentration over the southern flank and adjacent slope to increase with increasing salinity and with decreasing temperature, a trend apparent in each of the 3 years in which the nutrient data were acquired.

[23] When superimposed on the nutrient contours of this plot, the T-S properties of the intrusions seen in August fall in areas of negligible nitrate plus nitrite concentrations (<3 μmo L^{-1}) (Figure 9). By contrast, the T-S properties of the May intrusion appear in areas of modest nitrate plus nitrite concentrations (5–8 μmo L^{-1}). However, the

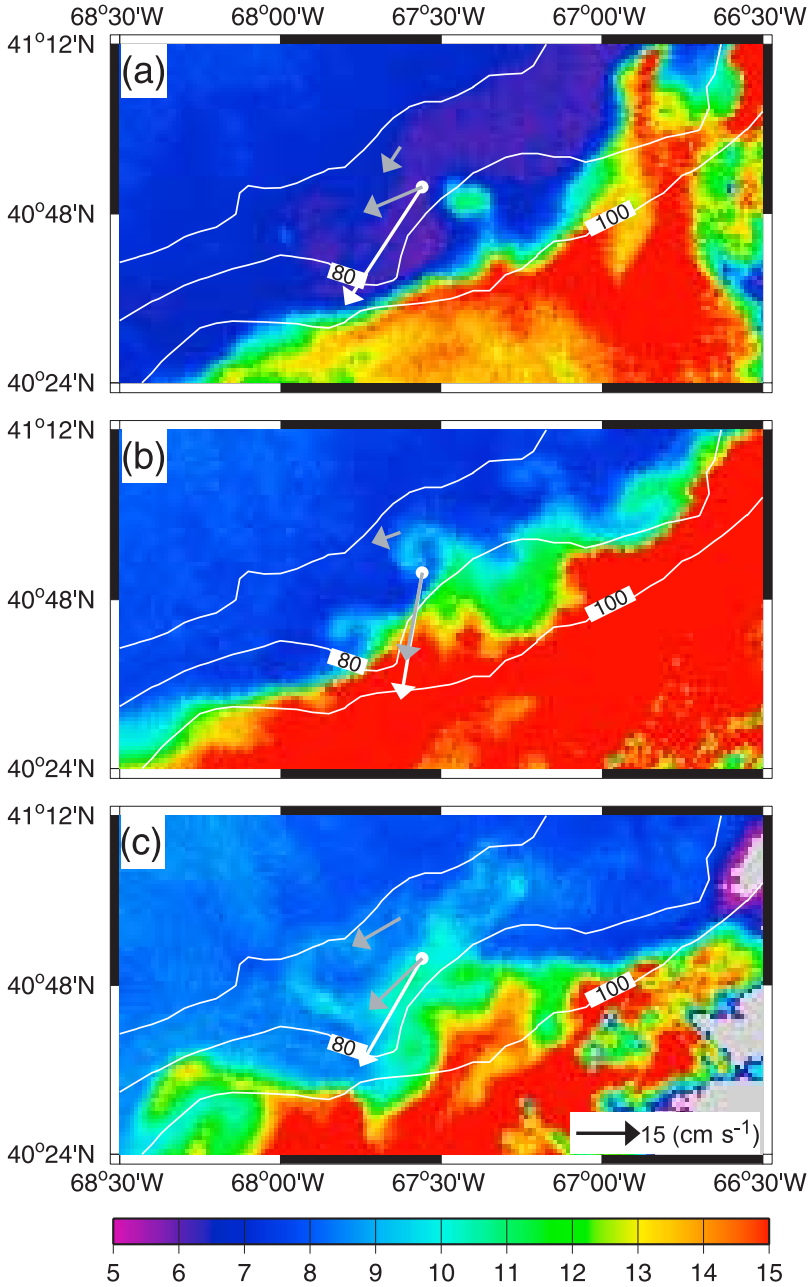

Figure 6. Sea surface temperature images showing small-scale warm-water features at the edge of the warm water intrusions on (a) May 6, (b) May 14, and (c) May 20, 1995. The velocity vectors are derived from low-pass-filtered velocity records from 5 and 31 m at ST1 (white and gray vectors, respectively) and from 31 m at ST2.

T-S properties of the resident flank water seen in May (with S < 32.5) appear over roughly the same range of nitrate plus nitrite concentrations (Figure 9, left). Similar patterns are seen when the T-S properties of the intrusions are superimposed on contour plots of silicate and phosphate.

[24] From these comparisons, two general conclusions may be deduced. One is that the upper water column intrusions of August were most likely nearly devoid of nutrients. The other is that the May intrusions, characterized by maximum salinities near the bottom, probably carried significant quantities of nutrients onto the southern flank, but at concentrations similar to nutrient concentrations of the resident southern flank water they displaced.

[25] Because of the limited data used to form the T-S-nutrient relationships, particularly at higher temperatures, the above conclusions must be viewed with some skepticism. Nevertheless, they are consistent with our examination of the 1997–1999 GLOBEC nutrient data, which reveals seven instances in which high salinity (>34) intrusions appear on the southern flank.

[26] Nutrient concentrations observed within near-surface (upper 20 m) warm (T > 16°C) intrusions are uniformly

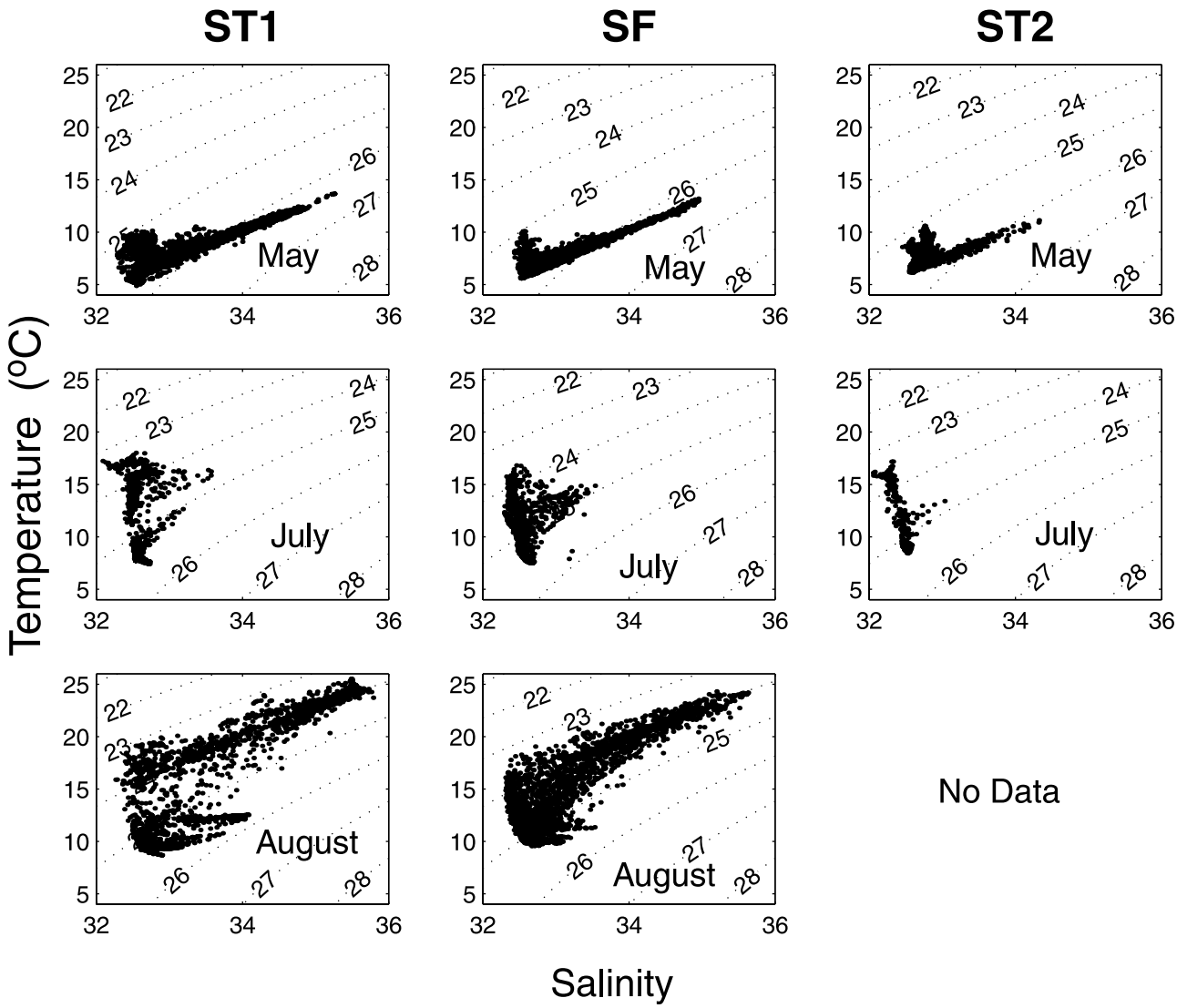

Figure 7. Temperature-salinity values measured at each mooring site during the times of the May, July, and August intrusions. For each intrusion and site, the values are from unfiltered temperature and salinity records (all records included) and span the period when elevated salinities of the intrusion appear in at least one of the site's salinity records.

low, not exceeding 0.5 μmo L^{-1} in nitrate plus nitrite and not greater than 0.2 μmo L^{-1} in phosphate (eight samples total). In the example shown here, from June 1999, the nitrate plus nitrite concentrations observed within the upper 20 m of a saline intrusion are significantly lower than near-surface nitrate plus nitrite concentrations measured elsewhere on the southern flank (Figure 10, top).

[27] Although nutrient concentrations within near-bottom intrusions are significant (4–12 μmo L^{-1} in nitrate plus nitrite, for example), there is no clear evidence that they tend to be greater than near-bottom nutrient concentrations measured elsewhere on the southern flank. As a rule, the nutrient concentrations observed in near-bottom intrusions fall within the range of nutrient concentrations measured within the same depth range elsewhere on the southern flank, as exemplified here by May 1999 nitrate plus nitrate data (Figure 10, bottom).

[28] To further assess the possible influence of high-salinity intrusions on nutrient concentrations over the southern flank, we used the 1997–1999 GLOBEC nutrient data to determine average nutrient versus depth profiles within the regions of the southern flank and the adjacent slope. This was done by first segregating the samples into slope region (bottom depth >200 m) and southern flank region (bottom depth <130 m) sets and then averaging the nutrient concentrations each set over 10-m-depth bins. The same procedure was carried out with the salinity data acquired with each nutrient sample. The results (Figure 11) show that although the mean salinity profile of the southern flank and slope data sets differ significantly, there is no evidence that the nutrient concentrations at a particular depth tends to be greater in the slope region relative to the flank region. In fact, for phosphate concentrations the opposite tendency is indicated. Within most depth bins, the mean phosphate concentration of the southern flank samples is higher than mean phosphate concentration of the slope samples. For nitrite plus nitrate, the difference between southern flank and slope

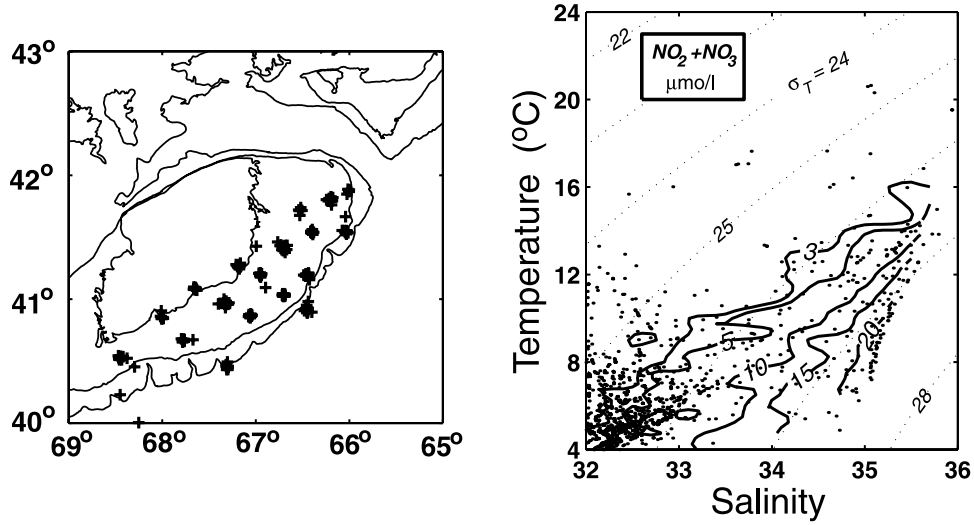

Figure 8. (right) Contours of constant nitrate plus nitrite concentration on a temperature and salinity surface, with points used to generate the contours superimposed. The contours were derived from data acquired at the stations (left) during 15 cruises conducted over 1997–1999 and during the months from January through June.

samples averages is small for all depth bins, significant above the 90% confidence level for only one bin. However, all averaged nutrient versus depth profiles tend to sharply increase with depth. It would seem reasonable, therefore, that slope water intrusions are more likely to result in an increase of nutrient concentration over the southern flank if their movement onbank includes upward vertical motion.

4.2. Intruding Eddies and Meanders

[29] As noted in section 3.2, SST imagery reveals numerous small-scale meanders at the edge of the August and

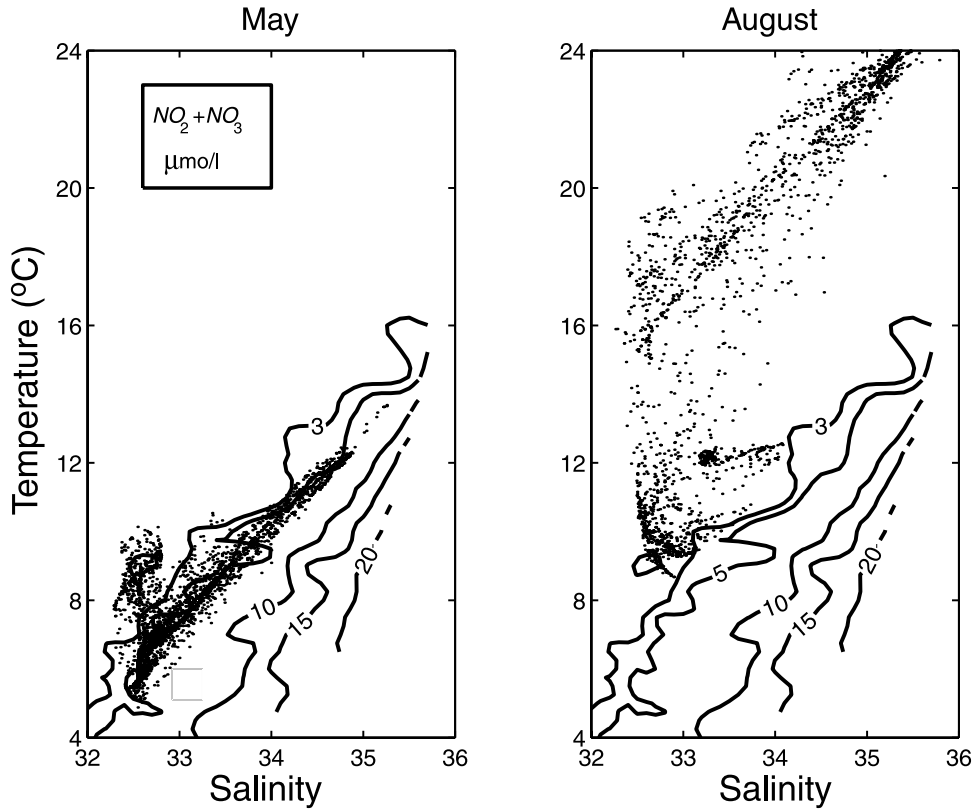

Figure 9. Temperature-salinity values measured at ST1 during the times of the May and August intrusions superimposed on the nitrate plus nitrite contour plot of Figure 8.

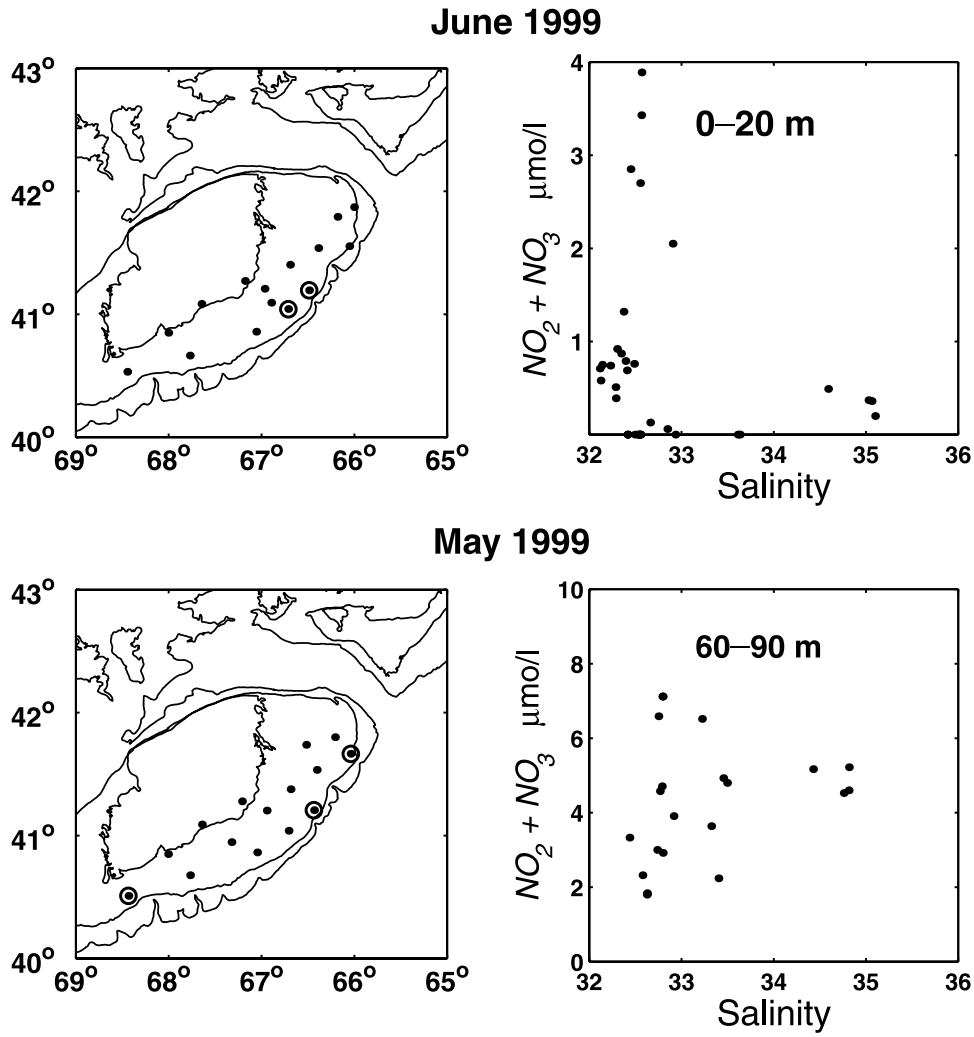

Figure 10. Nutrient concentrations measured during two cruises when high-salinity intrusions appeared on the southern flank. (left) Southern flank stations occupied during the indicated cruises with the stations at which saline intrusions (S > 34) were observed are circled. (right) Nitrate plus nitrate concentrations measured over the southern flank for the indicated cruise and depth range. Note that the June 1999 data show a near-surface intrusion with relatively low nitrate plus nitrite concentrations and the May 1999 data show a near-bottom intrusion with nitrate plus nitrite concentrations comparable to near-bottom nitrate plus nitrite concentrations found elsewhere on the southern flank.

May intrusions, as well as what appear to be detached eddies of intruding water. One may expect the signature of these eddies and meanders to be apparent in the moored instrument measurements. For example, a cyclonic eddy moving across a mooring site to the west (direction of the mean flow during the study period) should be evidenced by offbank flow followed by onbank flow. The velocity reversal should approximately mark the passage of the eddy's center directly onbank or offbank of the site. It should also nearly correspond to the maximum anomalies of temperature, salinity, and density. Westward passage of a meander crest at the edge of the intruding water would be expected to produce roughly the same pattern. This pattern is clearly evident in the ST1 measurements of the two intrusions appearing at the site during mid-May (Figure 3). In particular, the first intrusion produces a maximum salinity anomaly and a velocity reversal on May 16, and second intrusion gives similar features on May 21. For both intrusions, the salinity maximum coincides with a temperature maximum and with a maximum in density (Figure 12). If a near-geostrophic balance were in effect within the intrusion, the baroclinic pressure field about this density maximum would be accompanied by a cyclonic velocity field.

[30] The few cloud-free SST images of mid-May suggest that the first intrusion may be part of a small-scale meander, or possibly an eddy, passing ST1. Clear images are available for May 14, the day when the intrusion first appears at ST1. Apparent in these images is a warm, sharply crested meander with its western edge near the mooring site (Figure 6b). Later images suggest that the second intrusion may also be due to the passage of a meander crest. This is most clearly evidenced by the image of 1200 UTC May 20 (Figure 6c), acquired ~12 hours before the appearance of

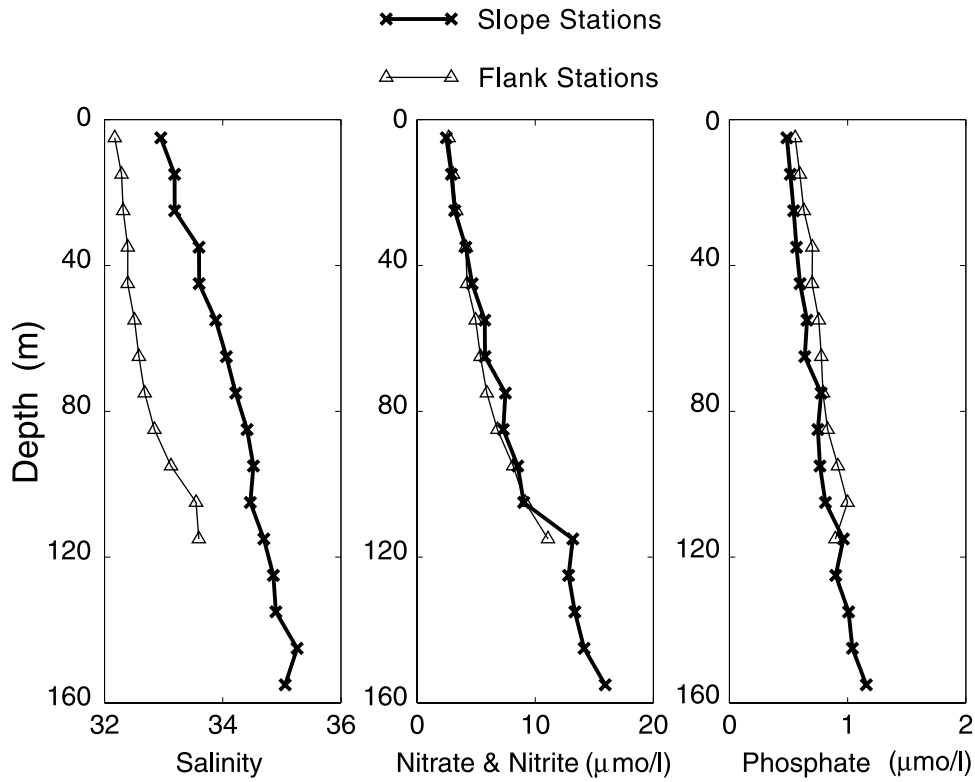

Figure 11. Profiles of averaged salinity and nutrient concentrations against depth for the regions of the southern flank and the adjacent slope. Averages were computed within 10-m-depth bins using the 1997–1999 GLOBEC nutrient-salinity data (Figure 8).

the second salinity maximum at ST1. In this image, ST1 appears to be immersed within the crest of a meander extending onto the bank.

[31] The limited measurements at ST2 (Figure 13) give an indication of the onbank extent of the intrusions seen in the ST1 data. Particularly illuminating are the ST2 salinity data from 11 and 32-m. These depths are within the vertical range of the intrusions' velocity signature as seen in the data from ST1 (Figure 3). During the time of the first intrusion's passage of ST1 (May 13–19), the 11- and 32-m salinity records at ST2 exhibit only a brief and small (order 0.25) salinity rise, suggesting that the intrusion may have extended onbank as far as ST2, but not much farther. This is consistent with the SST evidence of the intrusion (Figure 6b). During the passage of the second intrusion, the 11- and 32-m ST2 salinity records show no noticeable increase, indicating that this eddy had not penetrated as far onbank as ST2.

4.3. Cross-Margin Salt Fluxes

[32] To help judge the extent to which the intrusions may have impacted the cross-margin transport of water at the edge of the southern flank, we have used the ST1 salinity and velocity data to compute cross-bank salinity fluxes. These were defined as the flux of salinity in excess of the salinity of resident southern flank water; specifically,

$$F_S = u(S - S_o),$$

where F_S is the cross-bank transport of "excess" salinity, u is the cross-bank component of velocity, S is salinity, and S_o is the characteristic salinity of resident southern flank water. F_S may be converted to a salt flux by multiplying by water density. On the basis of the salinities measured at ST1 over the period of April–August with intrusions absent, S_o was set to 32.5.

[33] Fluxes occurring during the intrusions of May and August dominate the salinity flux time series as defined above (Figure 14). With all five flux time series considered, variation of flux during the times of these intrusions account for 90% of the overall flux variance.

[34] While our data are not adequate to judge the extent to which the intrusions may have produced a net transport of salinity onto the bank, some insight may be gained by examining the net flux of salinity of an intrusion event. Here we consider only the mean fluxes of the May intrusions, as these are the only intrusions of high salinity (>34) water fully encompassed by the mooring data. The salinity signature of the August intrusion is still apparent at the end of the ST1 time series.

[35] In the upper 47 m, the mean salinity fluxes of the May intrusions are all much smaller than their standard errors (Table 2). The indication is that the eddy, or meander, features that constituted the May intrusions in the upper water column passed the mooring site with no appreciable net transfer of salt onto the bank, or at least no net transfer that could be determined with statistical confidence with our measurements. Such a statement cannot be made with full certainty for the near-bottom intrusions of May, which did not exhibit the structure of an eddy or meander. At 65 m, the mean flux of salinity over the designated May intrusion period is slightly greater than its standard error. This mean

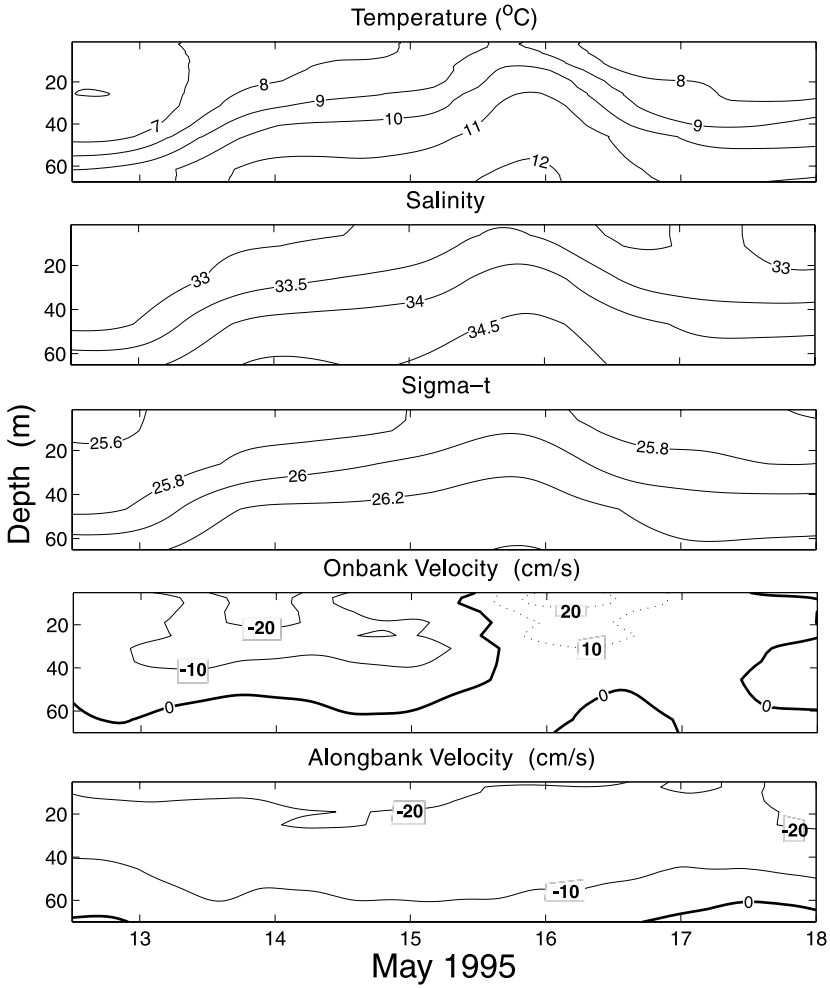

Figure 12. Water properties and velocities measured at ST1 during the passage of an intrusion during mid-May 1995.

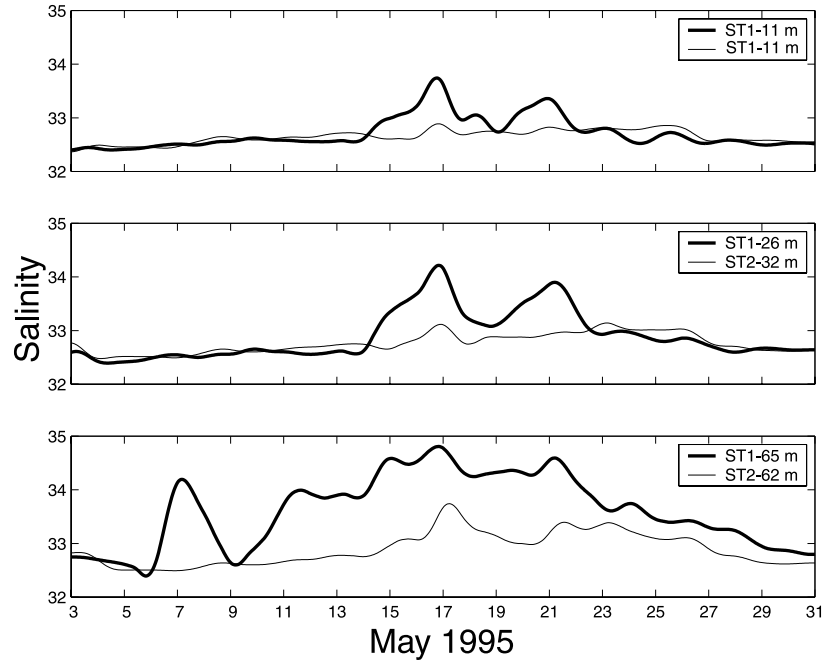

Figure 13. Low-pass filtered time series of salinity at the indicated depths at ST1 and ST2 during May 1995.

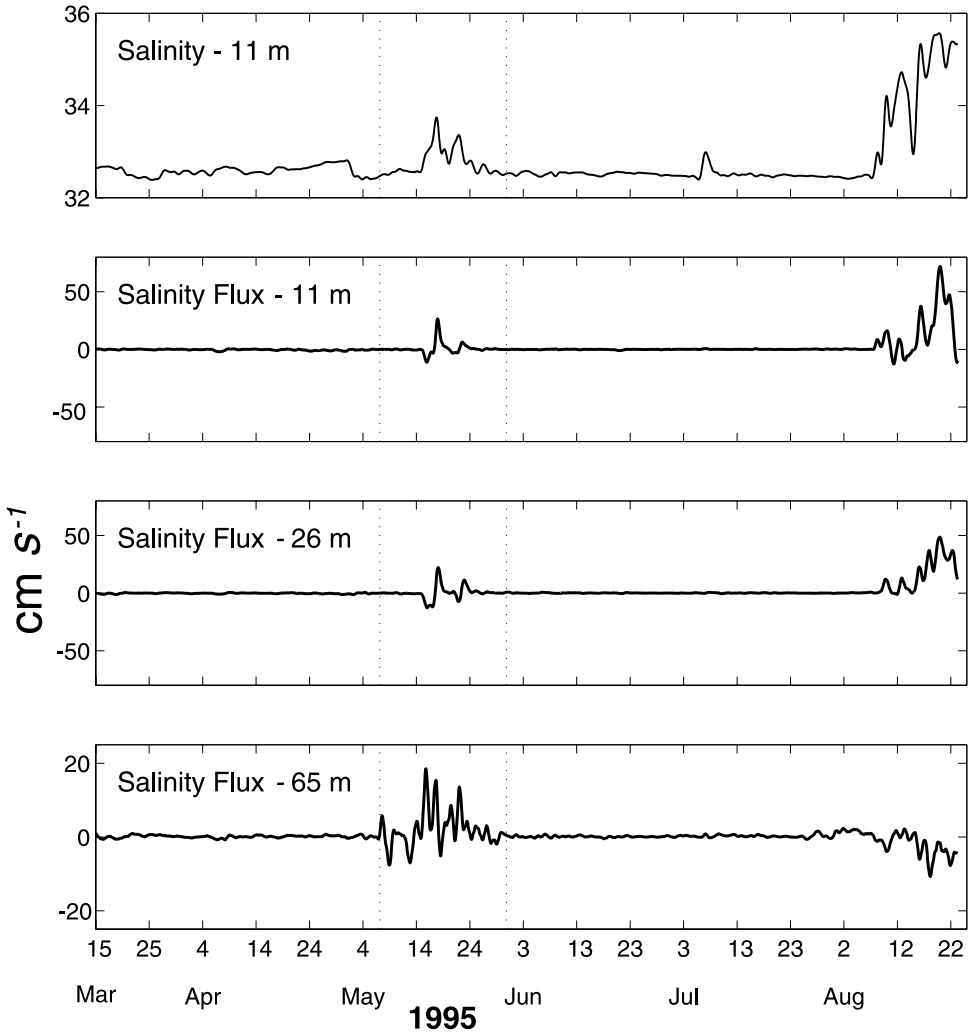

Figure 14. (top) Salinity at 11 m and (bottom three panels) the cross-margin flux of salinity in excess of the "resident" southern flank water salinity. The fluxes were computed from low-pass-filtered salinity and velocity records measured at the indicated depths at site ST1. Positive flux is directed onbank. The vertical dashed lines bracket the period over which the intrusion averaged fluxes of Table 2 were computed.

flux is significantly different from zero at the 80%, but not at the 90%, confidence level (Table 2). Most of this mean flux (roughly 90%) is due to the product of mean onshore velocity and mean excess salinity over the intrusion period (Table 2).

4.4. Impact of Wind Forcing

[36] Assessing the impact of wind forcing on the movement of the intruding water onto the bank can be partially accomplished by an examination of the wind stress, salinity, and cross-bank velocity time series (Figures 3 and 4). These indicate that wind-forced currents play an insignificant role in the appearance of the two full water column intrusions seen in May, which appear at ST1 during May 15–24. Both develop during a time when winds are particularly weak, with estimated stresses of <0.5 dynes cm^{-2}. More importantly, neither of these intrusions appears to be carried to ST1 by cross-bank currents as both first appear in the ST1 salinity records when the cross-bank currents measured at the site are directed offbank.

[37] Unlike the records of May, the ST1 measurements of August (Figure 4) give some evidence of wind-driven transport of high-salinity water onto the bank. The wind stress series of August is dominated by two events of strong wind stress with large along-bank components directed to the southwest. These occur over August 6–9 and 18–21, with the latter being the result of the passage of tropical storm Felix. The near-surface Ekman transport associated with the along-bank components of these wind events would be directed onbank. Indeed, both wind events correspond with episodes of strong near-surface onbank currents in the ST1 velocity records. These currents extend from the surface to at least 30 m depth and reach magnitudes in excess of 10 cm s^{-1}. The first saline intrusion seen in the August ST1 and SF salinity records appears near the end of the first storm, and could well be the result of onbank transport due to the wind-driven flow. However, the relationship of the second storm (Felix) with the appearance of intruding water is not clear cut. During this storm's passage, a saline intrusion appears at SF on August 20. At ST1,

Table 2. Means Over the Indicated Period of Cross-Bank Salinity Flux, Cross-Bank Velocity, and Excess Salinity at Site ST1[a]

Period, GMT	Depth, m	Mean Velocity, cm s^{-1}	Mean Excess Salinity	Excess Salinity Flux, cm s^{-1}	
				Mean	Standard Error[b]
0300 May 7 to 2000 May 30	6	−3.8	0.2	0.4	±1.1
	11	0.4	0.3	0.6	±1.3
	26	−0.2	0.5	0.3	±1.4
	47	−0.1	0.8	0.6	±1.0
	65	1.5	1.3	2.1	±1.3

[a]Positive fluxes and cross-bank velocities are directed onbank.
[b]Standard errors were computed as Std. Err. = $SD/(n_F)^{1/2}$, where SD is the standard deviation of the fluxes about the estimated mean and n_F are the number of independent flux measurements from which the mean was calculated; n_F was approximated as T/T_C, where T is the length of the flux series of the intrusion event and T_C is the correlation timescale of the flux series. On the basis of autocorrelation functions of the flux series, T_C was set to 40 hours. This was roughly the average integral timescale of the flux autocorrelation functions (integral of the function to the first zero crossing). The 80 and 90% confidence intervals about each estimated mean are roughly a factor of 1.35 and 1.75, respectively, of the range given by the standard error.

however, a saline intrusion is already present before the storm's arrival, and it is unclear if the storm alters this intrusion in any way. In addition, the saline intrusions that appear at SF and ST1 during the period of weak winds between the storms are not likely to be the result of onbank transport by wind-driven currents.

5. Discussion

[38] Because SST fields and our mooring data analysis show that high-salinity intrusions onto the southern flank often take the form of small-scale irregularly shaped frontal meanders and eddies, it is of interest to consider what may have generated such features. A prime candidate is instability of the shelf-edge frontal jet. Flowing in an equatorward direction over continental margin of Georges Banks and the Middle Atlantic Bight, this jet has been the object of several recent studies [*Linder and Gawarkiewicz*, 1998; *Pickart et al.*, 1999; *Fratantoni et al.*, 2001]. Baroclinic instability of the jet has been indicated by theoretical studies [*Gawarkiewicz*, 1991; *Lozier et al.*, 2002] and observations [*Linder and Gawarkiewicz*, 1998]. ADCP data acquired during May 1995 show the jet situated over the outer portion of the southern flank with a maximum velocity of 40–55 cm s^{-1}, and an across-bank extent of 15–20 km (Figure 15).

[39] In a recent numerical study, *Morgan* [1997] examines the formation of growing frontal meanders over the southern flank of Georges Bank arising from instability of the frontal jet. His case studies include typical winter and summer bank-edge fronts together with the front seen in the May 4, 1995, CTD-ADCP section (Figure 15). According

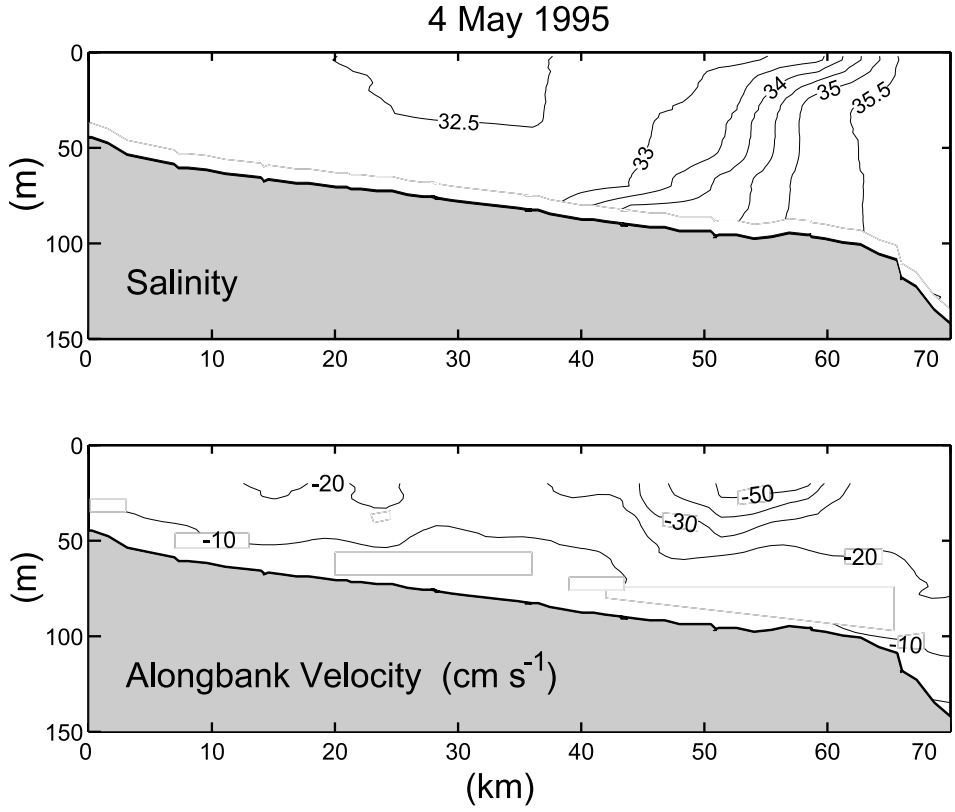

Figure 15. Fields of salinity and sub-tidal along-bank velocity measured across the southern flank on May 4, 1995. See Figure 5 for locations of measurement lines.

to his results, the doubling time of the fastest growing instability of the May 4, 1995, front is only 0.8 day. This is considerably shorter than the 3–6 day doubling times of unstable modes of the typical winter and summer fronts. His findings indicate that the most unstable mode of the May 1995 front is highly baroclinic and has a wavelength of 30 km. This compares favorably with the baroclinic nature of the meanders observed in mid-May, although their wavelength in the SST field appears to be somewhat longer, of order 50 km.

[40] Morgan hypothesizes that the shelfbreak front of May 1995 is particularly unstable due to the interaction of the front with the nearby warm-core ring (Figure 5). It is worth noting that SST images show a warm-core ring at the bank-edge to the northeast of all intrusions examined in this study. The impact of warm-core rings on the generation of frontal meanders is the subject of a modeling study by *Sloan* [1996]. He examines flow and water mass exchange at the shelf-edge front of the Middle Atlantic Bight with rings in various locations offshore of the shelf-edge and with no ring present. The results indicate that frontal instabilities may form in the absence of a ring, but that a ring tends to enhance eddy-driven intrusions onto the shelf.

[41] The extent to which frontal meanders and eddies effect a net transfer of slope water to the southern flank has yet to be resolved. Our finding that the frontal meanders observed by the May 1995 data from ST1 passed the mooring without a statistically resolved net flux of salt onto the southern flank is consistent with the analysis of *Lentz et al.* [2003]. From a careful examination of the salt balance on Georges Bank over February–August 1995, they conclude that the May intrusions passed along the southern flank with no observable residual impact on the salinity within the SF-ST1-ST2 triad of moorings.

[42] One of the most significant potential impacts of the movement of offbank water onto the southern flank is the delivery of high nutrient concentrations from the slope region. The data we examined do not show unusually high nutrient concentrations within high-salinity intrusions, as compared with nutrient concentrations in the same depth range elsewhere on the southern flank. However, because of the limited quantity of data examined, we cannot confidently state that the slope water intrusions may never enhance nutrient concentrations over the southern flank. In particular, given the tendency for nutrient concentrations to increase with depth over the southern flank and adjacent slope, it is reasonable to speculate that intrusions whose onbank translation includes upward motion could significantly increase nutrient concentrations over the southern flank shelf.

[43] Another potentially important impact of intrusions on the southern flank is their effect on the relative distribution of various fish species. In separate studies, *Garrison et al.* [2001] and *Manning et al.* [2001] found evidence suggesting that several key species, including cod and haddock larvae, appeared to have been displaced onbank in response to the May 1995 intrusions. *Garrison et al.* [2001] examined species distributions of 10 surveys conducted over three separate years. Their analysis revealed an unusually high degree of spatial overlap between cod larvae and one of their primary predators, Atlantic herring, in the waters onbank of the May 1995 intrusions. They noted that conditions favorable for contact between larvae and their predators may also bring larvae and their prey into relatively close proximity.

6. Conclusions

[44] A notable feature of the intrusions seen in the 1995 Georges Bank data is their variability. On the basis of the depth of maximum salinity, three different types of intrusions are observed: near-bottom intrusions in May, a pycnocline intrusion in July, and a mix of pycnocline and near-surface intrusions in August. The data also show large short-term (order days) variations in the cross-bank flow and vertical salinity structure of the intruding waters. Our analysis has indicated that these are due in part to wind-driven motions, principally in August. Meanders and eddies formed at the edge of the intruding water are also shown to be important contributors to these variations. The May data show the westward passage of two cyclonic features, each with a core of intruding water. Previous model results have implicated instability of the along-bank jet over the outer flank as the likely cause of meanders and eddies seen at the edge of the intruding water, and suggest that the nearby presence of warm-core rings may enhance eddy formation. Although our analysis has not revealed evidence that intrusions significantly increase nutrient concentrations over the southern flank, the possibility the intrusions may carry nutrients in relatively high concentrations to the southern flank cannot be discounted.

[45] **Acknowledgments.** We are especially grateful to G. Gawarkiewicz and S. Lentz for numerous helpful discussions during the course of our study and for critical reading of this manuscript. The manuscript was significantly improved through the suggestions of two anonymous reviewers. Our thanks go to M. Caruso for work on processing the Georges Bank mooring data and for generating the images seen in Figures 5 and 6. We are particularly grateful to the late Carol Alessi for her untiring efforts on data processing and analysis throughout the course of the U.S. GLOBEC NW Atlantic/Georges Bank program. The work carried out at WHOI was supported by the U.S. National Science Foundation under grants OCE-98-06498, OCE-96-32357, OCE98-06397, and OCE02-27679. The effort at the Woods Hole NMFS was funded through a grant from the NOAA Coastal Ocean Program. WHOI contribution 10649, U.S. GLOBEC contribution 403.

References

Alessi, C., et al., The 1995 Georges Bank Stratification Study moored array measurements, *Tech. Rep. WHOI-01-11*, 101 pp., Woods Hole Oceanogr. Inst., Woods Hole, Mass., 2001.

Beardsley, R. C., S. J. Lentz, R. A. Weller, R. Limeburner, J. D. Irish, and J. B. Edson, Surface forcing on the southern flank of Georges Bank, February–August 1995, *J. Geophys. Res.*, *108*(C11), 8007, doi:10.1029/2002JC001359, in press, 2003.

Boicourt, W. C., and P. W. Hacker, Circulation on the Atlantic continental shelf of the United States, Cape May to Cape Hatteras, *Mem. Soc. R. Sci. Leige*, *10*, 187–200, 1976.

Churchill, J. H., and F. Aikman III, The impact of fine particles discharged at the 106-Mile Municipal Sewage Sludge Dump Site, *J. Mar. Environ. Eng.*, *2*, 181–202, 1996.

Churchill, J. H., P. C. Cornillion, and G. W. Milkowski, A cyclonic eddy and shelf-slope water exchange associated with a Gulf Stream warm-core ring, *J. Geophys. Res.*, *91*, 9615–9623, 1986.

Dean, J. P., and R. C. Beardsley, A vector-averaging wind recorder (VAWR) system for surface meteorological measurements in CODE, *Tech. Rep. WHOI-88-20*, 68 pp., Woods Hole Oceanogr. Inst., Woods Hole, Mass, 1988.

Flagg, C. N., Hydrographic structure and variability, in *Georges Bank*, edited by J. H. Ryther and J. W. Farrington, pp.108–124, MIT Press, Cambridge, Mass., 1987.

Flagg, C. N., and M. Dunn, Characterization of the mean and seasonal flow regime on Georges Bank from shipboard acoustic Doppler current pro-

filer data, *J. Geophys. Res.*, *108*(C11), 8002, doi:10.1029/2001JC001257, in press, 2003.

Flagg, C. N., R. W. Houghton, and L. J. Pietrafesa, Summertime thermocline and sub-thermocline cross-frontal intrusions in the Mid-Atlantic Bight, *Deep Sea Res., Part II*, *41*, 325–340, 1994.

Fratantoni, P. S., R. S. Pickart, D. J. Torres, and A. Scotti, Mean structure and dynamics of the shelfbreak jet in the Middle Atlantic Bight during fall and winter, *J. Phys. Oceanogr.*, *31*, 2135–2156, 2001.

Garrison, L. P., W. Michaels, J. S. Link, and M. J. Fogarty, Predation risk on larval gadids by pelagic fish in the Georges Bank ecosystems: I. Spatial overlap associated with hydrographic features, *Can. J. Fish. Aquat. Sci.*, *57*, 2455–2469, 2001.

Gawarkiewicz, G., Linear stability models of shelfbreak fronts, *J. Phys. Oceanogr.*, *21*, 471–488, 1991.

Gordon, A. L., and F. Aikman III, Salinity maximum in the pycnocline of the Middle Atlantic Bight, *Limnol. Oceanogr.*, *26*, 123–130, 1981.

Hare, J. A., and R. K. Cowen, Expatriation of *Xyrichtys novacula* (*Pisces: Labridae*) larvae: Evidence of rapid cross-slope exchange, *J. Mar. Res.*, *49*, 801–823, 1991.

Hare, J. A., and R. K. Cowen, Transport mechanisms of larval and pelagic juvenile bluefish (*Pomatomus saltatrix*) from the South Atlantic Bight spawning grounds to Middle Atlantic Bight nursery habitats, *Limnol. Oceanogr.*, *41*, 1264–1286, 1996.

Houghton, R. W., and J. Marra, Physical/biological structure and exchange across the thermohaline shelf/slope front in the New York Bight, *J. Geophys. Res.*, *88*, 4467–4481, 1983.

Houghton, R. W., C. N. Flagg, and L. J. Pietrafesa, Shelf-slope water frontal structure, motion and eddy heat flux in the southern Middle Atlantic Bight, *Deep Sea Res., Part II*, *41*, 273–306, 1994.

Lentz, S., R. C. Beardsley, R. Weller, J. Manning, J. Irish, K. Brink, and P. C. Smith, Temperature and salt balances on Georges Bank, February–August 1995, *J. Geophys. Res.*, *108*(C11), 8006, doi:10.1029/2001JC001220, in press, 2003.

Linder, C. A., and G. Gawarkiewicz, A climatology of the shelfbreak in the Middle Atlantic Bight, *J. Geophys. Res.*, *103*, 18,405–18,423, 1998.

Lozier, M. S., M. S. C. Reed, and G. Gawarkiewicz, Instability of a shelfbreak front, *J. Phys. Oceanogr.*, *32*, 924–944, 2002.

Manning, J. P., R. G. Lough, C. E. Naimie, and J. H. Churchill, Modelling the effect of a slope-water intrusion on advection of fish larvae in May 1995 on Georges Bank, *ICES J. Mar. Sci.*, *58*, 985–993, 2001.

Morgan, D. T., Linear instability of the shelfbreak front off the southern flank of Georges Bank, Ph.D. thesis, Dartmouth Coll., Hanover, N. H., 1997.

Pickart, R. S., D. J. Torres, T. K. McKee, M. J. Caruso, and J. E. Prystup, Diagnosing a meander of the shelf break current in the Middle Atlantic Bight, *J. Geophys. Res.*, *104*, 3121–3132, 1999.

Sloan, N. Q., III, Dynamics of a shelf-slope front: Process studies and data-driven simulations in the Middle Atlantic Bight, Ph.D. thesis, Harvard Univ., Cambridge, Mass., 1996.

R. C. Beardsley and J. H. Churchill, Department of Physical Oceanography, Woods Hole Oceanographic Institution, Woods Hole, MA 02543, USA. (rbeardsley@whoi.edu; jchurchill@whoi.edu)

J. P. Manning, National Marine Fisheries Service, National Oceanic and Atmospheric Administration, Woods Hole, MA 02543, USA. (jmanning@whsun1.wh.whoi.edu)